INSTITUTE OF PHYSICS PUBLISHING JOURNAL OF OPTICS B: QUANTUM AND SEMICLASSICAL OPTICS
J. Opt. B: Quantum Semiclass. Opt. **6** (2004) 444–447 PII: S1464-4266(04)84547-6

Rotary dipole-mode solitons in Bessel optical lattices

Yaroslav V Kartashov[1,2], Alexey A Egorov[2], Victor A Vysloukh[3] and Lluis Torner[1]

[1] ICFO-Institut de Ciencies Fotoniques and Department of Signal Theory and Communications, Universitat Politecnica de Catalunya, 08034 Barcelona, Spain
[2] Physics Department, M V Lomonosov Moscow State University, 119899 Moscow, Russia
[3] Departamento de Fisica y Matematicas, Universidad de las Americas, 72820 Puebla, Mexico

Received 4 August 2004, accepted for publication 6 September 2004
Published 17 September 2004
Online at stacks.iop.org/JOptB/6/444
doi:10.1088/1464-4266/6/11/003

Abstract
We address Bessel optical lattices of radial symmetry imprinted in cubic Kerr-type nonlinear media and show that they support families of stable dipole-mode solitons featuring two out-of-phase light spots located in different lattice rings. We show that the radial symmetry of the Bessel lattices affords a variety of unique soliton dynamics including controlled radiation-free rotation of the dipole-mode solitons.

Keywords: optical lattices, solitons

The basic features of propagation of optical radiation in media with transverse modulation of the refractive index are known to depart considerably from those for uniform media. Local refractive index maxima with appropriate characteristics form waveguides that enable self-trapping and guiding of light beams. When the refractive index is modulated periodically, thus creating an array of evanescently coupled waveguides, the formation of discrete solitons is possible in the neighbouring array sites [1, 2]. Discrete solitons exhibit a number of unique features including controllable steering and switching that make them promising to demonstrate all-optical routing concepts [3]. Here we study the intermediate regime encountered in lattices with variable refractive index modulation depth, capable of operating in both regimes of weak and strong coupling between neighbouring sites [4, 5]. The concept behind such a regime might be termed *tunable discreteness*, with the strength of modulation being the parameter that tunes the system properties from predominantly continuous to predominantly discrete. In recent landmark experiments it was shown that lattices with flexibly controlled refractive index modulation period and depth can be induced optically [6–10]; this exhibits a number of advantages in comparison with the technological fabrication of evanescently coupled waveguide arrays. The properties of lattice solitons supported by such types of periodic lattices are being comprehensively investigated (see [4–16]).

The possibilities afforded by the lattices for soliton control depend crucially on the lattice overall symmetry. In particular, the periodicity of lattices dictates the band-gap structure of the existence domain for lowest-order solitons and their low-power asymptotical profiles (Bloch waves); it also defines the permitted configurations of soliton arrays, and the symmetry of the corresponding field distributions (e.g., quasi-discrete vortices). Therefore, a wealth of new possibilities is open, in both optics and matter wave fields, by lattices of radial symmetry created with non-diffracting Bessel beams. Those feature a cylindrical symmetry, thus new phenomena that are non-accessible with periodic (pixel-like) lattices. In this paper we address the unique possibilities afforded by Bessel lattices. In particular we introduce families of dipole-mode spatial solitons supported by a Bessel optical lattice imprinted in a focusing cubic nonlinear medium and perform their stability analysis. We show that such dipole-mode solitons are stable upon propagation above a minimum power threshold, and we illustrate the concept of the controlled rotation and reorientation of the dipole-mode solitons by an auxiliary control beam.

We consider the propagation of optical radiation along the z-axis in a bulk cubic medium with transverse modulation of the linear refractive index described by a nonlinear Schrödinger equation for dimensionless complex field amplitude q:

$$i\frac{\partial q}{\partial \xi} = -\frac{1}{2}\left(\frac{\partial^2 q}{\partial \eta^2} + \frac{\partial^2 q}{\partial \zeta^2}\right) + \sigma q\,|q|^2 - pR(\eta,\zeta)q. \qquad (1)$$

Here the longitudinal ξ and transverse η, ζ coordinates are scaled to the diffraction length and input beam width,

respectively, and $\sigma = \mp 1$ stands for the focusing/defocusing nonlinearity. Parameter p is proportional to the depth of refractive index modulation. Here we consider the case of the simplest radial Bessel lattice described by $R(\eta, \zeta) = J_0[(2b_{\rm lin})^{1/2}(\eta^2 + \zeta^2)^{1/2}]$, where $b_{\rm lin}$ defines the radii of the lattice rings [17], and leave more complicated lattices, including those with azimuthal modulation, for future consideration. Notice that the function $q(\eta, \zeta, \xi) = J_0[(2b_{\rm lin})^{1/2}(\eta^2 + \zeta^2)^{1/2}] \exp(-{\rm i}b_{\rm lin}\xi)$ gives an exact solution of the linear homogeneous equation (1) at $\sigma = p = 0$, and describes non-diffracting two-dimensional laser beams, in close analogy with the intersecting planar waves used for lattice formation in [6–10]. We assume that the depth of refractive index modulation is small compared with the unperturbed refractive index and is of the order of the nonlinear contribution. Notice that equation (1) admits several conserved quantities including the energy flow U, the Hamiltonian H, and the longitudinal projection of the angular momentum $\mathbf{L}$:

$$U = \int_{-\infty}^{\infty}\int_{-\infty}^{\infty} |q|^2 \, {\rm d}\eta \, {\rm d}\zeta,$$

$$H = \int_{-\infty}^{\infty}\int_{-\infty}^{\infty} \left(\frac{1}{2} |\nabla q|^2 + \frac{\sigma}{2} |q|^4 - pR\,|q|^2 \right) {\rm d}\eta \, {\rm d}\zeta, \quad (2)$$

$$L_\xi = \mathbf{L}\mathbf{e}_\xi = \frac{\mathbf{e}_\xi}{2{\rm i}} \int_{-\infty}^{\infty}\int_{-\infty}^{\infty} [\mathbf{r} \times (q^* \nabla q - q \nabla q^*)] \, {\rm d}\eta \, {\rm d}\zeta.$$

Here $\nabla = \mathbf{e}_\eta(\partial/\partial\eta) + \mathbf{e}_\zeta(\partial/\partial\zeta)$ is the differential operator acting in the transverse plane, $\mathbf{r} = \mathbf{e}_\eta\eta + \mathbf{e}_\zeta\zeta$ is the radius vector of the point with coordinates (η, ζ), and $\mathbf{e}_\eta$, $\mathbf{e}_\zeta$, $\mathbf{e}_\xi$ are unitary vectors in the directions η, ζ, ξ, respectively.

We search for soliton solutions in the form $q(\eta, \zeta, \xi) = w(\eta, \zeta) \exp({\rm i}b\xi)$, where $w(\eta, \zeta)$ is a real function and b is a real propagation constant. Soliton families are defined by the propagation constant b, the parameter $b_{\rm lin}$, and the lattice depth p. Since scaling transformations $q(\eta, \zeta, \xi, p) \to \chi q(\chi\eta, \chi\zeta, \chi^2\xi, \chi^2 p)$ can be used to obtain various families of lattice solitons from a given one, here we set the transverse scale in such way that $b_{\rm lin} = 10$, and vary b and p. In this paper we concentrate only on focusing nonlinear media with $\sigma = -1$, although we verified that defocusing Bessel lattices also support localized solitons. Linear stability analysis of the solitons was carried out by searching for the perturbed solutions $q(\eta, \zeta, \xi) = [w(\eta, \zeta) + u(\eta, \zeta, \xi) + {\rm i}v(\eta, \zeta, \xi)] \exp({\rm i}b\xi)$, with u and v being the real and imaginary parts of the perturbation which can grow with complex growth rate δ. A standard linearization procedure for equation (1) yields a system of coupled equations for the perturbation components u, v:

$$\begin{aligned} \frac{\partial u}{\partial \xi} &= -\frac{1}{2}\left(\frac{\partial^2 v}{\partial \eta^2} + \frac{\partial^2 v}{\partial \zeta^2} \right) + bv - w^2 v - pRv, \\ -\frac{\partial v}{\partial \xi} &= -\frac{1}{2}\left(\frac{\partial^2 u}{\partial \eta^2} + \frac{\partial^2 u}{\partial \zeta^2} \right) + bu - 3w^2 u - pRu. \end{aligned} \quad (3)$$

This system was solved numerically with a split-step Fourier method in order to find the perturbation profiles and the corresponding growth rates.

First we consider dipole-mode solitons that intuitively can be viewed as a nonlinear superposition of out-of-phase soliton beams supported by the central core and the first lattice ring. Because of the repulsive interaction between the out-of-phase beams, such localized states cannot exist in the absence of a Bessel lattice. The lattice compensates the repulsion and leads to stationary propagation. The typical profile of a stationary dipole-mode soliton calculated from equation (1) by relaxation method is presented in figure 1(a). From now on, these solutions will be referred to as centred dipole-mode solitons. The energy flow of a centred dipole-mode soliton is a non-monotonic function of the propagation constant b, as shown in figure 1(b). At high energy flows the dipole-mode soliton transforms into a pair of narrow non-interacting bright solitons. When $b \to \infty$, the total energy flow tends to twice the energy of the so-called Townes soliton. There exists a lower cutoff $b_{\rm co}$ on the propagation constant that is a non-monotonic function of the lattice depth (figure 1(c)). Close to the lower cutoff the dipole-mode solitons become spatially extended and cover several lattice rings. At approximately $p \leqslant 8.2$ centred dipole-mode solitons cease to exist at the lower cutoff without any topological transformation, while at $p > 8.2$ centred dipole-mode solitons transform into radially-symmetric solutions that appear as a bright central peak surrounded by concentric rings with the shape of the linear guided mode of a radially symmetric Bessel lattice. This transformation of the asymptotical soliton shapes corresponds to the discontinuity in the $b_{\rm co}(p)$ dependence (figure 1(c)). Notice that with growth of p the part of the soliton energy carried out by the core decreases, and at $p \to \infty$ most of the soliton energy is concentrated in the first lattice ring.

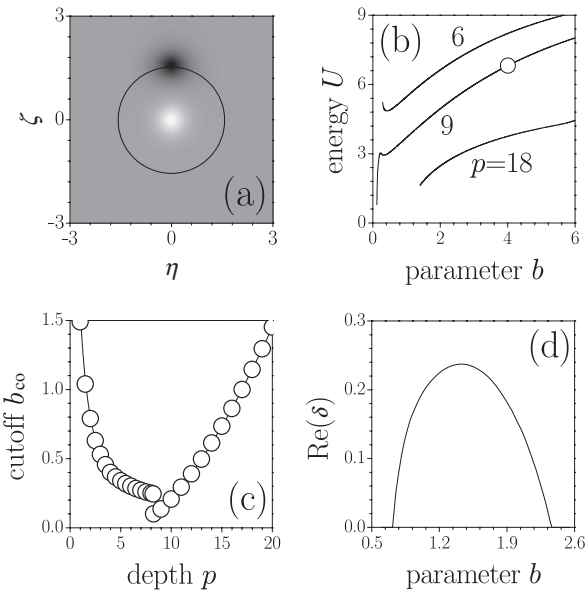

Figure 1. (a) Profile of a centred dipole-mode soliton corresponding to the point marked by the circle in dispersion diagram (b). (c) Cutoff on propagation constant versus lattice depth. (d) Real part of perturbation growth rate versus propagation constant at $p = 9$.

Our stability analysis revealed that the centred dipole-mode solution becomes free of linear instabilities above a certain energy flow threshold (above the corresponding critical value of the propagation constant). The instability domain is located near the cutoff and the corresponding perturbation growth is of oscillatory type (figure 1(d)). Our calculations

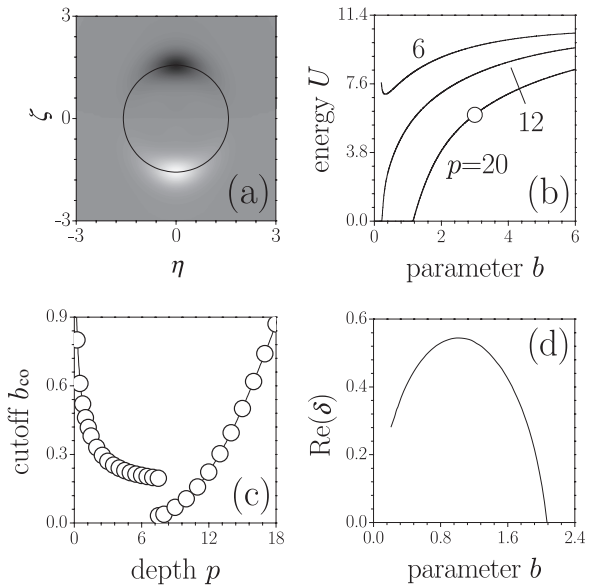

Figure 2. (a) Profile of a ring dipole-mode soliton corresponding to the point marked by the circle in dispersion diagram (b). (c) Cutoff on propagation constant versus lattice depth. (d) Real part of perturbation growth rate versus propagation constant at $p = 6$.

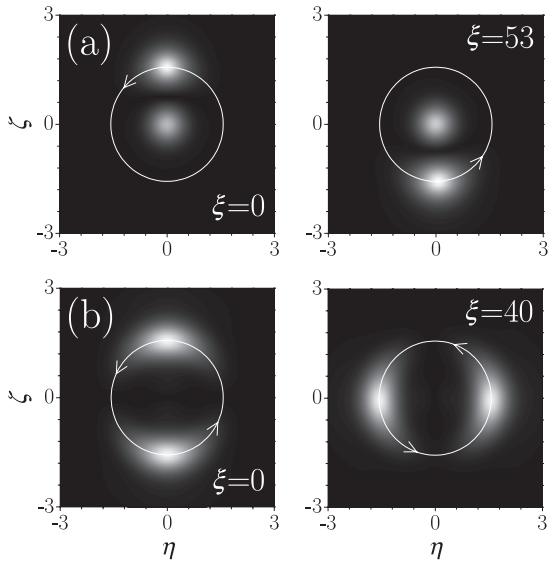

Figure 3. Induced rotation of centred (a) and ring (b) dipole-mode solitons in a Bessel lattice. The soliton shown in row (a) corresponds to $b = 4$ at $p = 9$. The soliton component trapped in the first lattice ring is set in rotary motion by launching it tangentially to lattice ring at an angle $\alpha = 0.1$. The soliton shown in row (b) corresponds to $b = 3$ at $p = 20$. Both components are set in rotary motion by imposing initial phase twist $\nu = 0.1$.

reveal that the width of the instability region reduces when the lattice depth grows. Close to the cutoff we found complex narrow stability bands, whose detailed study falls beyond the scope of this paper; thus we do not display them in figure 1(d).

Besides the centred dipole-solitons discussed above, we have found a new type of dipole-mode solitons, which are supported by the first lattice ring (figure 2(a)). Those will be referred to as ring dipole-mode solitons. At approximately $p > 7.5$ such solitons transform into linear waves at the lower cutoff, and their energy flow vanishes, while at $p \leqslant 7.5$ the ring dipole-mode ceases to exist at the cutoff without any topological transformation (figure 2(b)). As in the case of centred solitons, this is accompanied by a discontinuity of the $b_{co}(p)$ dependence (figure 2(c)). At high energy flows the two beams forming the ring dipole-mode solitons become very narrow, while at low energies they spread over the first lattice ring (figure 1(a)), so that their overlap becomes high. The same behaviour is encountered with growth of the lattice depth at fixed energy flow.

The linear stability analysis shows that ring dipole-mode solitons also turn out to be completely stable above the energy flow threshold (figure 2(d)). The instability band is located near the lower cutoff, and its width decreases with growth of the lattice depth so that at $p = 20$ ring dipole-mode solitons become stable almost in the entire domain of their existence. It should be mentioned that at a critical stabilization value of the propagation constant, the two beams forming the ring dipole-mode soliton still overlap considerably. This indicates that stabilization is due to the lattice. Notice that inside the instability bands both oscillatory and exponential instabilities occur with ring dipole-mode solitons.

The central new possibilities open by the Bessel lattices are linked to their radial symmetry, which makes it possible to set solitons, and in particular dipole-mode solitons, into controlled rotation. Rotation of the so-called centred dipole-mode solitons can be achieved by launching one component trapped in the first lattice ring tangentially to the ring at an angle α. Ring dipole-mode solitons can be set into rotary motion by imposing on them an initial phase twist $\exp(i\nu\phi)$, where ϕ is the azimuth angle and ν stands for the so-called winding number or phase twist (figure 3). In contrast to solitons supported by periodic lattices, that always radiate energy upon their motion across the lattice because they ought to overcome opposing potential across the lattice [3], rotating dipole-mode solitons in Bessel lattices do not radiate. This property of solitons supported by Bessel lattices gives rise to a number of unique interaction types.

For example, the symmetry axis of the dipole-mode solitons can jump upon the action of an additional control beam launched into the second lattice ring. If the energy flow of the control beam largely exceeds that of the dipole-mode solitons, the control beam does not experience considerable displacement upon interaction, while the axis of the dipole-mode solitons can rotate up to 180°. This concept is illustrated in figure 4, where the arrows show the direction of reorientation of the dipole-mode soliton axis and the direction of displacement of the control beam. The control beam is out of phase with the dipole-mode soliton located in the first lattice ring. The direction of the rotation and its rate are dictated by the position of the control beam, and by the relative phase between the control beam and the dipole-mode soliton. Notice that nonlinearity is necessary for the observed behaviour throughout the paper, because even though linear guided modes analogous to the ring dipole-mode solitons that we describe here can in principle be supported by linear Bessel lattices, their rotation is always accompanied by radiation losses.

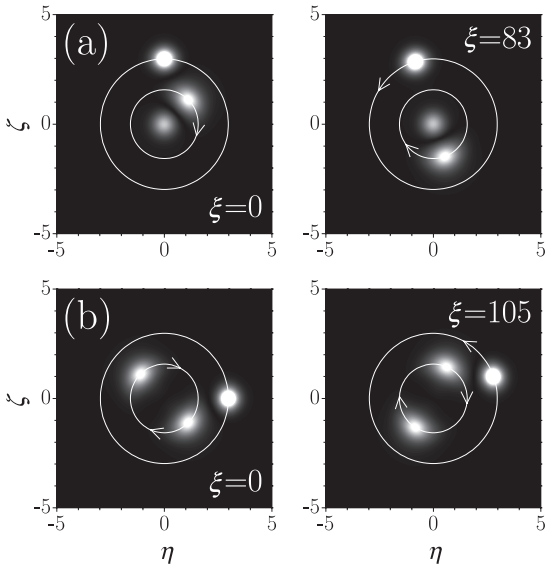

Figure 4. Reorientation of centred (a) and ring (b) dipole-mode solitons under the action of a high-energy control soliton launched into the second lattice ring. Centred and ring dipole-mode solitons correspond to $b = 3$. The high-energy control soliton is taken at $b = 10$. Lattice depth $p = 9$.

In conclusion, we have revealed properties of two types of dipole-mode solitons supported by radially symmetric Bessel optical lattices in Kerr-type cubic nonlinear media. We showed that such solitons become completely stable above a minimum power threshold. Because of the radial symmetry of the lattice, we showed that the solitons can be set into controlled, radiation-free rotation, thus featuring a number of unique soliton dynamics.

Acknowledgments

This work has been partially supported by the Generalitat de Catalunya, and by the Spanish Government through grant BFM2002-2861.

References

[1] Christodoulides D N and Joseph R I 1988 *Opt. Lett.* **13** 794
[2] Eisenberg H S, Silberberg Y, Morandotti R, Boyd A R and Aitchison J S 1998 *Phys. Rev. Lett.* **81** 3383
[3] Christodoulides D N, Lederer F and Silberberg Y 2003 *Nature* **424** 817
[4] Kartashov Y V, Zelenina A S, Torner L and Vysloukh V A 2004 *Opt. Lett.* **24** 766
[5] Kartashov Y V, Torner L and Vysloukh V A 2004 *Opt. Lett.* **24** 1102
[6] Fleischer J W, Carmon T, Segev M, Efremidis N K and Christodoulides D N 2003 *Phys. Rev. Lett.* **90** 023902
[7] Fleischer J W, Segev M, Efremidis N K and Christodoulides D N 2003 *Nature* **422** 147
[8] Neshev D, Ostrovskaya E, Kivshar Y and Krolikowski W 2003 *Opt. Lett.* **28** 710
[9] Neshev D N, Alexander T J, Ostrovskaya E A, Kivshar Y S, Martin H, Makasyuk I and Chen Z 2004 *Phys. Rev. Lett.* **92** 123903
[10] Fleischer J W, Bartal G, Cohen O, Manela O, Segev M, Hudock J and Christodoulides D N 2004 *Phys. Rev. Lett.* **92** 123904
[11] Efremidis N K, Hudock J, Christodoulides D N, Fleischer J W, Cohen O and Segev M 2003 *Phys. Rev. Lett.* **91** 213906
[12] Yang J and Musslimani Z 2003 *Opt. Lett.* **28** 2094
[13] Kartashov Y V, Vysloukh V A and Torner L 2004 *Opt. Express* **12** 2831
[14] Musslimani Z and Yang J 2004 *J. Opt. Soc. Am.* B **21** 973
[15] Yang J, Makasyuk I, Bezryadina A and Chen Z 2004 *Opt. Lett.* **29** 1662
[16] Kartashov Y V, Egorov A A, Torner L and Christodoulides D N 2004 *Opt. Lett.* **29** 1918
[17] Kartashov Y V, Vysloukh V A and Torner L 2004 *Phys. Rev. Lett.* **93** 093904